Synthesis of oligosaccharide libraries from GBS capsular polysaccharides for structure-based selection of vaccine candidates

Del Bino, L.

Chapter 6

Characterization of sugar-mAb interactions of GBS serotype Ia and Ib oligosaccharides

Del Bino, L.; Carboni, F.; Romano, M.R.; De Ricco, R.; Brogioni, B.; Adamo, R. were involved in the research included in this Chapter.

Introduction

Bacterial cell surface carbohydrates are at the interface of multiple host-pathogen interactions and have been targeted to develop highly efficacious glycoconjugate vaccines against severe infections. Traditional glycoconjugate vaccines consist of long polysaccharides (obtained from bacterial sources) which are chemically conjugated to the carrier protein. Conjugation is performed through random linkage along the saccharide chain, resulting in the formation of high molecular weight, cross-linked heterogeneous structures[1-3].

To understand the mechanism of action of this type of vaccines, mapping of the epitopes recognised by functional antibodies, that mediate protection from infection, is crucial. In the absence of structural information, long oligosaccharides have to be employed to fully cover all of the relevant glycotopes[4]. An understanding of the structural basis for the immune recognition of carbohydrate epitopes and the elucidation of minimal saccharide antigens responsible for an effective immune response is relevant to support the rational design of modern glycoconjugate vaccines with well-defined synthetic oligosaccharides[5, 6].

Chemically assembled oligosaccharides would result in easier characterization of the corresponding glycoconjugates, lack of bacterial contaminants, higher reproducibility and more robust correlation of the immune response to the chemical structure of the saccharide[7].

Among GBS serotypes, the most studied is type III, that is known to form a helical structure[8, 9], and this feature has an impact on epitope exposure[9]. Recently CPSIII oligosaccharides have been synthesized and used along with fragments obtained from CPS depolymerization to map a sialylated structural epitope spanning two repeating units[6, 10]. The same approach could be theoretically applied also to other GBS serotypes such as Ia and Ib, which share with GBS III the same residue composition of the repeating unit[11], in order to define the glycotopes interacting with protecting mAbs. Since neither chemical nor enzymatic depolymerization reactions are available for CPS Ia and Ib, structurally defined oligosaccharides can be obtained only by chemical and/or enzymatic synthesis.

In Chapter 4 and 5 the synthesis of a panel of oligosaccharide fragments from GBS type Ia and Ib CPS has been described. Availability of these fragments allow for the first time a study of the interactions with anti CPS monoclonal antibodies to gain information on the structure of the minimal glyco epitope. Moreover, NMR studies can help to understand whether the specificity of the immune response observed for the two serotypes can be correlated to a different conformation.

As described in Chapter 4 and 5, NMR studies and molecular dynamics simulations highlighted a different conformational preference of GBS Ia polysaccharide compared to type Ib, with a particular effect in the orientation of the Neu5Acα2-3Gal branching (*exo-anti-Φ* for Ia and *exo-syn-Φ* for Ib). This reflects in a more repetitive and regular structure for PSIa, with the Neu5Ac exposed according to a well-defined spatial orientation, while PSIb has a more irregular, helix-shape backbone.

This different conformation is expected to influence antibody recognition.

In this Chapter, the study of the interactions of the library of synthesized oligosaccharides with serotype specific functional monoclonal antibodies is described. Competitive SPR, competitive ELISA and STD-NMR were performed with the aim to shed lights on the structural motif interacting with the mAb.

Finally, conjugates of the saccharides to the carrier protein CRM_{197} were prepared and characterized for future *in vivo* study and immunological evaluation.

Results

Competitive SPR of GBS type Ia and Ib oligosaccharides

The antigenicity of the synthesized GBS fragments was first assessed by competitive Surface Plasmon Resonance. The fragments included in the experiments are represented in Figure 1: four fragments from GBS serotype Ia CPS (the linear and branched repeating unit, **1** and **2** the Y-shape and the branched hexasaccharides **3** and **4**) and the two repeating unit frameshifts **5** and **6** from type Ib CPS. The capsular polysaccharides of both serotypes were included in each experiment as controls.

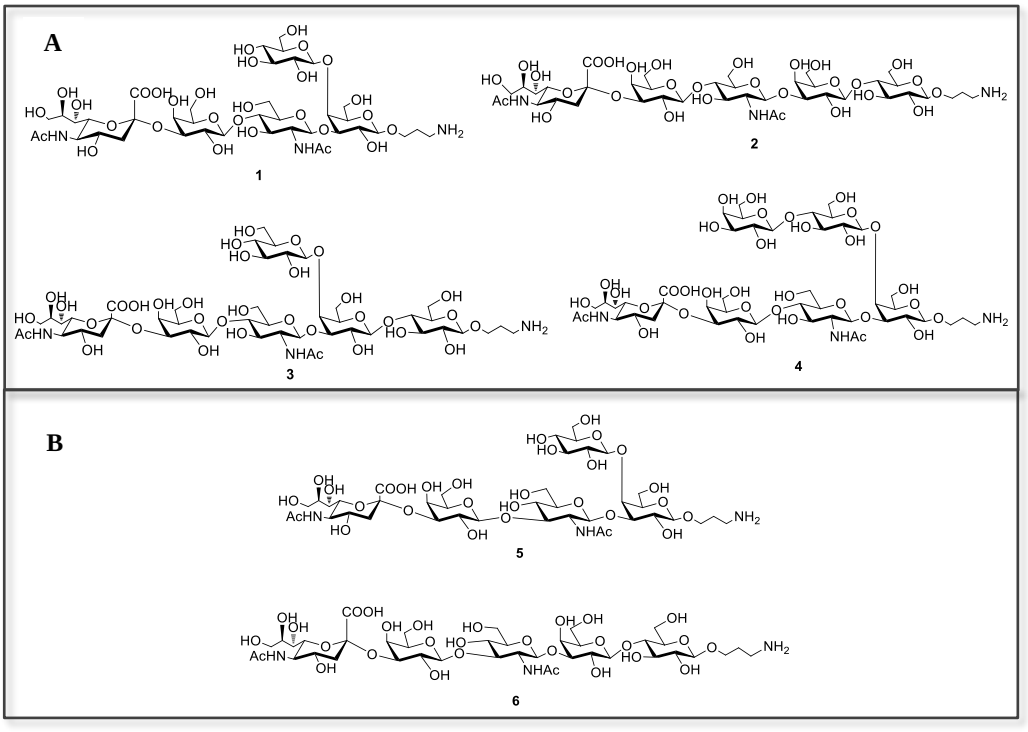

Figure 1. A) Oligosaccharide structures from GBS type Ia tested in competitive SPR. B) GBS type Ib repeating units tested in competitive SPR.

The structural features of the oligosaccharide determining antibody recognition were studied using two protective monoclonal antibodies raised in mice to PSIa and PSIb conjugates to CRM.
In the first experiment, the compounds **1**-**4** were used as inhibitors of the binding of the soluble murine anti PSIa mAb to a PSIa-Human Serum Albumin coniugate immobilized on a CM5 chip (Figure 2). PSIa was used as positive control, while PSIb and the branched Ib repeating unit **5** were the negative controls and were used to confirm that the mAb was non cross-reactive with serotype Ib.

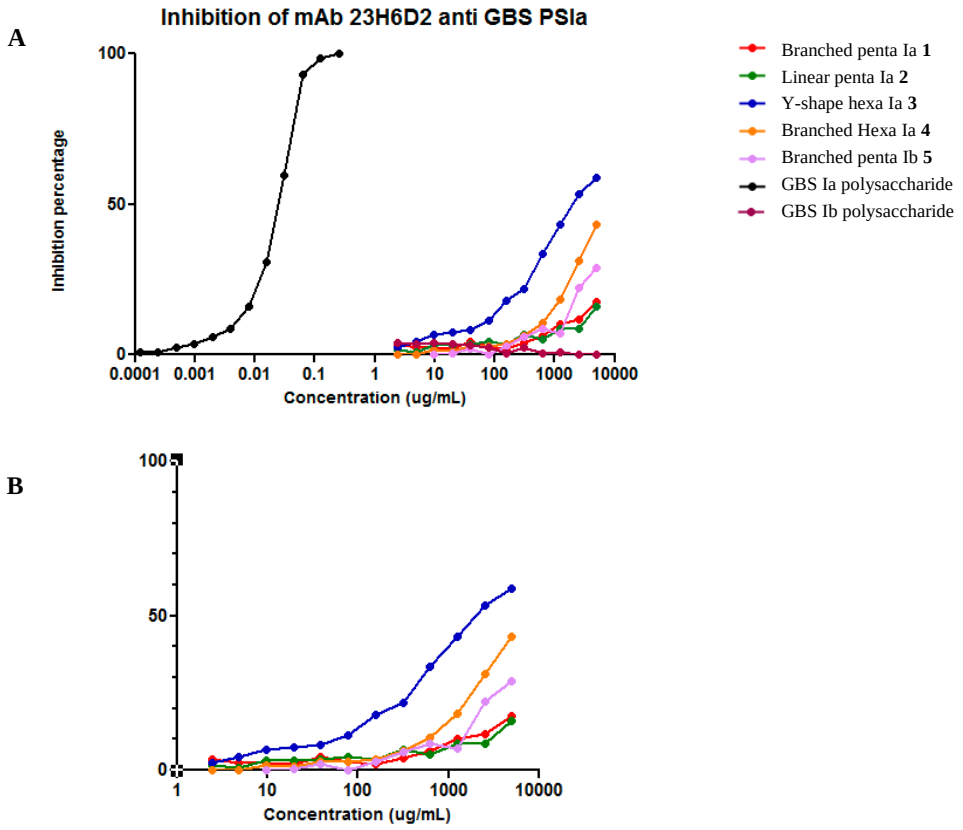

Figure 2. A) Competitive SPR vs anti PSIa murine monoclonal antibody 23H6D2. In black the Ia CPS used as positive control in the experiment. B) Enlargement on the synthetic fragments, showing the two hexasaccharides partially inhibiting the binding of the mAb to the immobilized PS.

Starting from a concentration of 5 mg/mL of each oligosaccharide, 2-fold serial dilution were made. GBS Ia pentasaccharide repeating units **1** and **2** failed completely to inhibit the binding. Only the hexasaccharides **3** and **4** were recognized by the murine protective mAb. Inhibition of binding was only partial even at the highest concentration, with the Y-shape hexasaccharide **3** being a slightly better inhibitor than the branched one (60% inhibition of **3** versus 45% of the branched structure **4**). As expected, the type Ib polysaccharide was not competing for binding to

the mAb with the PSIa. This confirmed that despite the high similarity between type Ia and Ib polysaccharide, the anti PSIa monoclonal antibody used was very specific and showed no cross reactivity. Interestingly, the branched repeating unit of GBS PSIb (**5**) was very weakly recognized by the mAb, better than the PSIb.

From these data it can be concluded that the synthesized GBS Ia fragments are not able to deplete the binding of type Ia polysaccharide to a monoclonal antibody anti PSIa. This indicates that they are not adequately covering the antigenic determinants required for antibody recognition. However, some differences can be observed in the affinity of the oligosaccharides to the mAb, with increasing binding affinity with increasing oligosaccharide size: in particular, the hexasaccharides **3** and **4** showed better inhibition activity compared to the pentasaccharides **1** and **2**. Additionally, when comparing short glycans and long polysaccharides, it has to be taken into consideration the higher avididy (re-binding) effect of the natural polymer, because of its exposure of many epitopes and this may explain the big affinity difference between the oligosaccharide fragments and the PSIa.

Next, the interactions of oligosaccharides **5** and **6** with an anti-PSIb mAb were investigated. To this aim, the two oligosaccharides, together with PSIb were used as inhibitors of the binding of the soluble anti PSIb mAb to PSIb conjugated to Human Serum Albumin and immobilized on a CM5 chip. PSIa and the branched hexasaccharide **4** were used as negative controls. The results, expressed as inhibition percentage of binding, indicate that both fragment **5** and **6** is recognized by the anti-PSIb mAb, with the branched repeating unit able to deplete the mAb recognition with a 2-log higher concentration compared to the positive control PSIb. A weaker inhibition (1-log difference) was detected with the linear structure **6**, suggesting that the arrangement of sugars in the RU impacts antibody recognition and the ramification point is relevant for binding (Figure 3). Finally, confirming the serotype-specificity of this mAb, PSIa was only very weakly recognized while the hexasaccharide **4** was not able to inhibit the binding.

IC_{50} values were calculated for PSIb and for both pentasaccharides **5** and **6** (Table 1). The branched pentasaccharide **5**, with an IC_{50} of 85.47 ug/mL, showed an affinity for the anti-PSIb mAb about 2-log lower with respect to the polysaccharide. As mentioned, the avidity effect due to the multivalent epitopes exposure can impact the binding of the polysaccharide. The calculated IC50 of the linear pentasaccharide **6** was 850.7 ug/mL, 1-log higher compared to the branched frameshift of the repeating unit, and this confirmed the importance of the ramification for mAb recognition and binding.

Figure 3. Competitive SPR vs anti PSIb murine monoclonal antibody

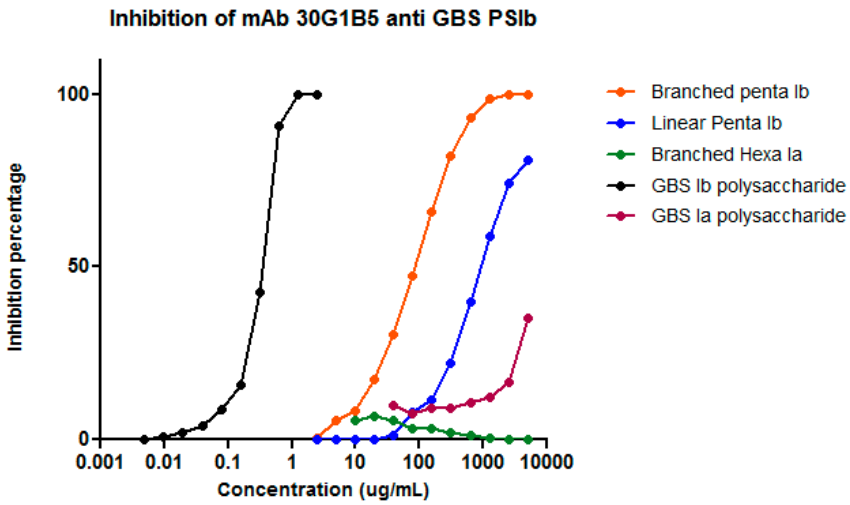

Table 1. IC50 for the interaction of mouse mAb with different glycans

Glycan	IC_{50} (µg/ml)
DP1 branched **5**	85.47
DP1 linear **6**	850.7
PSIb	0.58

STD-NMR of pentasaccharide 5

Considering the results obtained by competitive SPR, mapping of the interaction of the fragment with the protective mAb starting with the most promising compound **5** was commenced. To characterize the sugar/mAb interactions at the atomic level, Saturation Transfer Difference (STD-NMR) studies were undertaken[12, 13]. Indeed, STD experiments permit the deduction of interactions between a ligand (the sugar in this case) and a target receptor (the mAb) and, in favourable cases, the identification of the ligand epitope. STD NMR spectra of the pentasaccharide-mAb complex (ligand/protein 100:1 molar ratio) were derived by subtracting two different ^{1}H NMR spectra performed on the same sugar-mAb sample: the on-resonance, in which selective irradiation of protein protons is performed for a few seconds, and the off-resonance, which is recorded as a reference or blank spectrum. The obtained STD NMR spectrum only contains the ligand resonance whose intensities have been affected by the protein saturation. The experiment with a 1:100 mixture of mAb:pentasaccharide provided strong STD signals for the oligosaccharide (Figure 4).

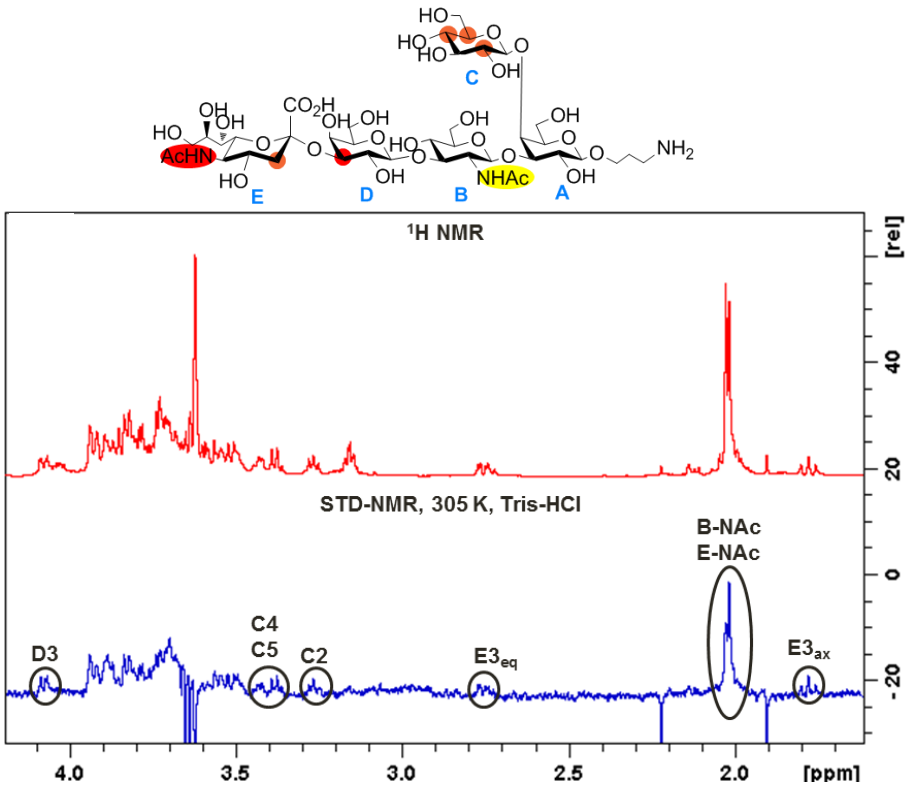

Figure 4. A) STD-NMR interpretation: mapping of the pentasaccharide protons closely interacting with the mAb; B) Off-resonance; C) STD-NMR of the complex pentasaccharide: anti PSIb mAb at 305 K, recorded at 600 MHz. Proton positions receiving strongest saturation after protein irradiation are circled in black.

Notably, most of the ^{1}H STD-NMR resonances that could unequivocally be assigned to the pentasaccharide **5**-mAb complex were related to the Glc residue of the backbone and the α-Neu5Ac-(2→3)-β-Gal-(1→4) residues, indicating a direct involvement of this branch.

Transfer of saturation was received especially by H_3-E equatorial and axial, H_3-D, H_2-C, H_4-C and H_5-C. Interestingly, only the acetamide on the sialic acid showed a high STD signal (76% of recovery versus 45% for the acetamide on the glucosamine), confirming the engagement of the Neu5Ac moiety in the binding to the mAb, while the backbone glucosamine seems to be involved to a lower extent. Notably, strong involvement of the side chain Neu5Ac and Gal sugars in the interaction with the corresponding anti PS mAb has been observed previously for GBS type III. In the GBS type Ib case, the STD-NMR pointed out that the Glc residue also plays a key role in the interaction with the mAb, indicating a direct involvement also of the backbone.

GBS glycans conjugates to CRM$_{197}$

In order to evaluate the immunogenicity of the synthetic oligosaccharides, selected fragments were conjugated to the classical carrier protein CRM$_{197}$. When it comes to the immunogenicity of

glycoconjugate vaccines, there are several parameters that can influence the immune response, among which, the type of protein carrier, the length of the saccharide antigen, the presence of charges, and the degree of carbohydrate loading[14]. In particular, for short glycans the saccharide/protein ratio has been shown to play a key role. Carboni at al. recently demonstrated that CRM conjugates of GBS type III oligosaccharides elicited higher antibody titers at increasing saccharide/protein ratio, with the influence of glycosylation degree being crucial for the shortest oligosaccharides[15]. For this reason, the aim was to obtain glycoconjugates with an average number of sugar chains per protein above 10 to understand whether multivalent exposure of sub-optimal epitopes could still result in an immune response in vivo.

Glycoconjugates of compounds **1**-**6** were conjugated to CRM_{197} taking advantage of the aminopropyl linker, which was activated by treatment with an excess of di-*N*-hydroxysuccinimidyl adipate[10]. The percentage of activation was monitored by NMR and the resulting activated ester was incubated with the carrier protein CRM_{197} in sodium phosphate buffer at pH 7.2. 75-100 equivalents of the active ester were used to obtain conjugates with a high glycosylation degree.

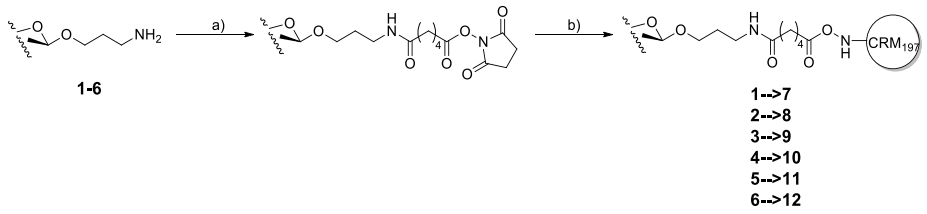

Scheme 1. *Reagents and conditions*: a) Di-*N*-hydroxysuccinimidyl adipate, triethylamine, DMSO; b) 0.8 M sodium phosphate 7.2.

The glycoconjugates were purified by filtration against sodium phosphate buffer and characterized by 3-8% sodium dodecyl sulfate polyacrylamide gel electrophoresis (SDS-PAGE) to estimate the carbohydrate/protein molar ratio and by microBCA to quantify the protein content. The degree of carbohydrate incorporation was then corroborated by quantification of the amount of galactose moieties present in the conjugated saccharide through high-performance anion-exchange chromatography coupled with pulsed amperometric detection (HPAEC-PAD). Apart from the conjugate CRM197-hexa Y-shape **9**, all the others reached the target of at least 10 saccharide chains per mol of protein as summarized in Table 1.

The reason why the CRM-hexa-Y shape conjugate **9** was obtained with a very low glycosylation degree was investigated retrospectively by analysis of the proton NMR spectra, which showed a very low activation percentage of the saccharide after treatment with di-*N*-hydroxysuccinimidyl adipate. This problem was caused by a reduced availability of the primary amine on the linker,

which was alkylated in the deprotection procedure, as confirmed after careful anaysis of the NMR and ESI-MS characterization of compound **3**.

Table 1. Attributes of the prepared glycoconjugates

Glycoconjugate	**mol NHS/ mol protein**	**Protein conc. (µg/mL)**	**Sacch. conc. (µg/mL)**	**Saccharide/protein ratio**
CRM_{197}-branched penta **7**	1:100	524	178.6	17:1
CRM_{197}-linear penta **8**	1:75	1245	342.1	14:1
CRM_{197}-hexa Y-shape **9**	1:75	257	5.9	1:1
CRM_{197}-hexa branched **10**	1:75	247	65.8	12:1
CRM_{197}-branched penta **11**	1:100	466	191.8	20:1
CRM_{197}-linear penta **12**	1:75	992	200.2	10:1

Western blot analysis with anti PSIa and PSIb monoclonal antibodies was performed on all conjugates (Figure 5 and 6). Unfortunately, none of the conjugates obtained with type Ia oligosaccharides were recognized by the mAb, confirming the results obtained by competitive SPR.

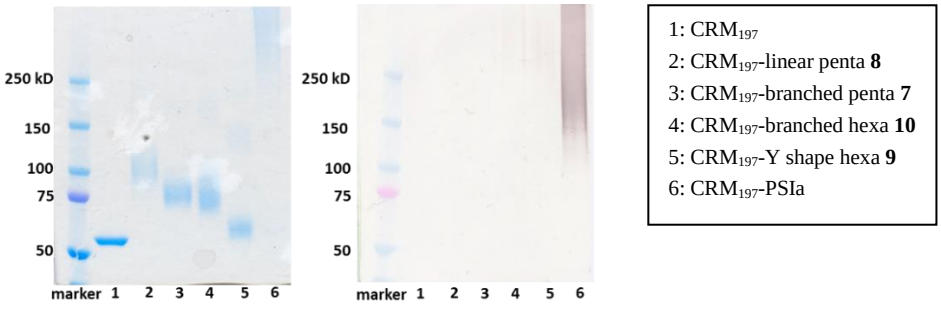

Figure 5. SDS-Page on GBS serotype Ia glycoconjugates and corresponding Western Blot

The Western Blot of GBS Ib oligosaccharide conjugates showed recognition only of the branched pentasaccharide repeating unit (compound **11**), confirming that the arrangement of the sugar residues in the repeating unit impacts antibody recognition.

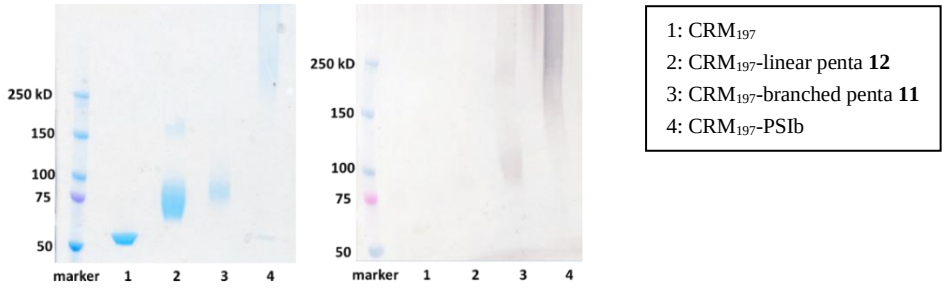

Figure 6. SDS-Page on GBS serotype Ib glycoconjugates and corresponding Western Blot

Overall, the data confirmed that GBS Ia and Ib capsular polysaccharides, despite a very similar chemical structure, present different carbohydrate epitopes. Monoclonal antibodies indeed show no cross-reactivity, not only with short fragments but also for the long polysaccharides. Moreover, while for GBS Ib a branched pentasaccharide is able to interact with an anti PSIb monoclonal antibody, longer structures from GBS Ia seem to be required for having a similar interaction.

Conclusion

The availability of structurally well-defined oligosaccharides is an essential requirement to gain information on structure-immunogenicity correlations of bacterial capsular polysaccharides and consequently to design better glycoconjugate vaccines[7]. When methods for the enzymatic and/or chemical depolymerization of the polysaccharide are not available, chemical synthesis is an essential alternative to obtain short oligosaccharides. GBS serotype Ia and Ib polysaccharides are typical examples of structures for which depolymerization is not applicable. For this reason, oligosaccharides **1**-**4** from GBS Ia and **5**-**6** from GBS Ib capsular polysaccharides were prepared and used to study their interactions with functional serotype specific murine mAbs. Competitive SPR confirmed that both monoclonal antibodies used were not cross-reactive towards the other GBS serotype. Unfortunately, GBS Ia oligosaccharides **1**-**4** were not able to deplete the binding of the anti PSIa mAb to the PSIa-HSA immobilized on a CM5 chip. This indicated that such short fragments are not covering the antigen involved in recognition by the anti-PSIa mAb used for the experiments. Most likely, longer oligosaccharides presenting more than one glucosamine and/or Neu5Ac moiety, are needed for full inhibition.

On the other hand, GBS Ib branched repeating unit **5** could fully deplete the binding of a soluble anti PSIb mAb to a PSIb-HSA conjugate immobilized on the chip. Recognition occurred also for the linear repeating unit **6**, with an IC50 1-log higher compared to compound **5**. The different recognition of the two frameshifts confirmed, as previously observed for GBS type III repeating unit[10], that the arrangement of the monosaccharide residues in the repeating unit is crucial to antibody recognition. To better map the interactions between the pentasaccharide and the mAb,

STD-NMR experiments were performed, highlighting that the α-Neu5Ac-(2→3)-β-Gal-(1→4) part is the most involved in the binding, as well as the Glc and the Gal of the backbone.
All the saccharides were then conjugated to CRM_{197} in order to evaluate their immunogenicity *in vivo*. The glycoconjugates were characterized in terms of protein and sugar content and a high carbohydrate loading was achieved for almost all compounds with the aim to compensate the poor immunogenicity of sub-optimal epitopes with their multivalent exposure. The conjugates will be tested in mice for their capability of eliciting specific anti-PSIa and anti-PSIb antibodies able to mediate opsonophagocytic killing (OPKA) of strains expressing type Ia and Ib PS respectively.

Experimental

SPR mAb binding inhibition

Inhibition assays were performed by SPR with a BIACORE X100 system using a CM5 sensor chip (Biacore) with immobilized HSA-PSIa or HSA-PSIb. Immobilizations were performed using the amine coupling kit supplied by the manufacturer (Biacore) and were conducted in 10-20 mM sodium acetate (pH 4-5) at sugar concentrations of 2-4 µg/mL. The immobilized surface density was ~50 resonance units in each instance. Measurements were conducted in 10 mM HEPES (pH 7.2), 150 mM NaCl, 3 mM EDTA, 0.005% Tween 20 at 25°C and at a flow rate of 45 µL/min. Following mAb binding, conjugate surfaces were regenerated with 3.5 M $MgCl_2$ and a contact time of 120 s. Binding analysis was performed with samples of mAb at a fixed concentration pre-incubated with PSIa/PSIb or their fragments serially diluted (2x) starting from a concentration of 5 mg/mL. Sensorgram data were analyzed using BIAevaluation software (Biacore).

Competitive ELISA

Microtiter plates (96 wells, NUNC, Maxisorp) were coated with 100 µL of 1 µg/mL of PSIa and PSIb capsular polysaccharide conjugated to Human Serum Albumin in PBS 1x. Plates were incubated overnight at 2–8°C, washed three times with PBST (0.05% Tween-20 in PBS pH 7.4) and saturated with 250 µL/well of PBST-B (2% Bovine Serum Albumin-BSA in PBST) for 90 min at 37 °C.

Two-fold serial dilutions of the oligosaccharide fragments and polysaccharide controls were incubated at rt for 30 min with anti PSIa and PSIb mice sera in PBST-B, then were added to each well and tested in duplicate. Plates were incubated at 37 °C for 1 h, washed with PBST, and then incubated for 1:30 h at 37 °C with anti-mouse IgG-alkaline phosphatase (Sigma) diluted 1:2000. After washing, the plates were developed with a 4 mg/mL solution of *p*-Nitrophenyl Phosphate (pNPP) in 1 M diethanolamine (DEA) pH 9.8, at rt for 30 min. After blocking with 7% EDTA, the absorbance was measured using a SPECTRAmax plate reader with wavelength set at 405 nm. Results were expressed as inhibition percentage of the anti PSIa and PSIb IgGs.

STD NMR experiments

NMR experiments were carried out on a Bruker 600 MHz NMR instrument equipped with a TBI cooled probe at controlled temperature (± 0.1 K). Data acquisition and processing were performed using TOPSPIN 1.3 and 3.1 software, respectively. Suppression of water signal was achieved by excitation sculpting (2 msec selective square pulse). Proton-Carbon Saccharides resonances were assigned collecting both 1D (^{1}H and ^{13}C) and 2D (TOCSY, NOESY, HSQC, HSQC-TOCSY) experiments, using standard pulse sequences. STD-NMR experiments were acquired with 96 scans over 96 accumulations and spectral width of 8000 Hz (12 ppm) at 305 K; a saturation transfer of 2/4 sec. was applied to enhance the saturation transfer effect, irradiating at a frequency of 7.5 and -0.5 ppm. To avoid pitfalls in the interpretation of STD-NMR spectra, a negative control spectrum was always recorded in absence of mAb (ligand and buffer) at the very same condition (concentration and pH) of the mAb-saccharide samples. The STD negative controls were always subtracted to the relative mAb-saccharide STD spectrum, obtaining the STDD experiments.

NMR sample preparation

mAb was exchanged in the working buffer (Tris d-11 50 mM in D_2O at pH 8.0 +/- 0.1) through 2 mL Zeba Spin desalting column saturated with 3 cycles of working buffer. mAb was finally eluted at the same starting concentration of 0.3 mg/ml. The 100% of recovery was assessed through microBCA spectrophotometric assay. The saccharides used was desalted, quantified, dried and then dissolved in the working buffer too. mAb final concentration in the NMR tube was of 3 µM. Ligand (saccharide):mAb ratio was set 100:1 mol/mol.

CRM_{197} conjugation of synthetic DPs

A solution of di-N-hydroxysuccinimidyl adipate (12 eq) and triethylamine (5 eq) in DMSO was added to compounds **1**-**6** to have a final concentration of 40 umol/mL of saccharide. The reaction was stirred for 3h, then the product was precipitate at 0°C by adding ethyl acetate (9 volumes). The solid was washed 10 times with ethyl acetate (5 volumes each) and lyophilized. The activated sugar was conjugated to CRM_{197} in sodium phosphate 0.8 M at a protein concentration from 23 to 42.6 mg/ml (depending on the sample), using a molar ratio of 75-100:1 saccharide/protein.

SDS-PAGE analysis

Sodium Dodecyl Sulfate- Polyacrylamide gel electrophoresis (SDS-PAGE) was performed on 3-8% pre-casted polyacrylamide gel (NuPAGE®Invitrogen) using tris acetate as running buffer (NuPAGE®Invitrogen). 5µg of protein were loaded for each sample. After electrophoretic running with a voltage of 150V for about 45 min, the gel was stained with blue Coomassie.

Western Blot analysis

SDS-Page was run as described before. Gel was transferred on cellulose with iBlot® gel transfer stacks nitrocellulose kit and blocked with PBS 1x pH 7.2+BSA 3%. Anti PSIa and PSIb mAbs were used as primary antibody (dilution 1:1000, 1 h) followed by 5 washes with PBS+tween 0,05% buffer. Anti-mouse IgG alkaline phosphatase was used as secondary antibody (dilution 1:2000, 30min) followed by 5 washes with PBS+tween 0,05% buffer. Western-Blot was finally developed with AP conjugate substrate kit (BIORAD®).

HPAEC-PAD analysis for revealing Gal, Glc and GlcNAc

Standard samples of GBS PSIa and PSIb at five increasing concentrations ranging between 0.5 and 10.3 µg/mL were prepared to build the calibration curve. GBS PSIa and Ib samples were prepared targeting the calibration curve midpoint. The reference and analytical samples were prepared in 4 M trifluoracetic acid, incubated at 100°C for 3h, dried under vacuum (SpeedVac Thermo), and suspended in water. All analytical samples were filtered with 0.45 µm Phenex-NY (Phenomenex) filters before analysis. HPAEC-PAD analysis was performed with a Dionex ICS-3000 equipped with a CarboPac PA1 column (4 × 250 mm; Dionex) coupled with a PA1 guard to column (4 × 50 mm; Dionex). Samples (50 µL injection volume) were run at 1 mL/min, using isocratic elution with 14 mM NaOH, followed by a washing step with 0.5 M NaOH.

HPAEC-PAD data acquisition and analysis

In HPAEC-PAD analysis, the effluent was monitored using an electrochemical detector in the pulse amperometric mode with a gold working electrode and an Ag/AgCl reference electrode. A quadruple-potential waveform for carbohydrates was applied. The resulting chromatographic data were processed using Chromeleon software 6.8 (Dionex). Gal, Glc, GlcNAc and Neu5Ac concentration were determined and converted in µmol/mL to estimate the relative mol/mol ratio.

References

1. Costantino, P.; Rappuoli, R.; Berti, F. *Expert Opin. Drug Dis.* **2011**, *6*, 1045-1066.
2. Khatun, F.; Stephenson, R.J.; Toth, I. *Chem. Eur. J.* **2017**, *23*, 4233-4254.
3. Ravenscroft, N.; Costantino, P.; Talaga, P.; Rodriguez, R.; Egan, W. **2015**, DOI: 10.1007/978-3-662-45024-6_8, 301-381.
4. Micoli, F.; Del Bino, L.; Alfini, R.; Carboni, F.; Romano, M.R.; Adamo, R. *Expert Rev. Vaccines*, **2019**, *18*, 881-895.
5. Anish, C.; Schumann, B.; Pereira, C.L.; Seeberger, P.H. *Chem. Biol.* **2014**, *21*, 38-50.
6. Carboni, F.; Adamo, R.; Fabbrini, M.; De Ricco, R.; Cattaneo, V.; Brogioni, B.; Veggi, D.; Pinto, V.; Passalacqua, I.; Oldrini, D.; Rappuoli, R.; Malito, E.; Margarit Y Ros, I.; Berti, F. *Proc. Natl. Acad. Sci. U. S. A.* **2017**, *114*, 5017-5022.
7. Adamo, R. *Accounts Chem. Res.* **2017**, *50*, 1270-1279.
8. González-Outeiriño, J.; Kadirvelraj, R.; Woods, R.J.; *Carbohyd. Res.* **2005**, *340*, 1007-1018.
9. Kuttel, M.; Ravenscroft, N. *Pharmaceuticals*, **2019**, *12*, 28.
10. Cattaneo, V.; Carboni, F.; Oldrini, D.; De Ricco, R.; Donadio, N.; Margarit Y Ros, I.; Berti, F.; Adamo, R. *Pure Appl. Chem.* **2017**, *89*, 855-875.
11. Jennings, H.J.; Katzenellenbogen, E.; Lugowski, C.; Kasper, D.L. *Biochemistry*, **1983**, *22*, 1258-1264.
12. Johnson, M.A.; Jaseja, M.; Zou, W.; Jennings, H.J.; Copie, V.; Pinto, B.M.; Pincus, S.H. *J. Biol. Chem.* **2003**, *278*, 24740-24752.
13. Johnson, M.A.; Pinto, B.M.; *Carbohyd. Res.* **2004**, *339*, 907-928.
14. Avci, F.; Berti, F.; Dull, P.; Hennessey, J.; Pavliak, V.; Prasad, A.K.; Vann, W.; Wacker, M.; Marcq, O. *mSphere*, **2019**, *4*, e00520-19.
15. Carboni, F.; Angiolini, F.; Fabbrini, M.; Brogioni, B.; Corrado, A.; Berti, F.; Adamo, R.; Margarit Y Ros, I. *J. Infect. Dis.* **2019**, DOI: 10.1093/infdis/jiz551.